Resonance Raman Studies of Oxo Intermediates in the Reaction of Pulsed Cytochrome *bo* with Hydrogen Peroxide†

Takeshi Uchida,‡ Tatsushi Mogi,§ and Teizo Kitagawa*,‡

Institute for Molecular Science, Okazaki National Research Institutes, Myodaiji, Okazaki 444-8585, Japan, and Department of Biological Sciences, Graduate School of Science, University of Tokyo, Hongo, Bunkyo-ku, Tokyo 113-0033, Japan

Received November 3, 1999; Revised Manuscript Received February 28, 2000

ABSTRACT: Cytochrome *bo* from *Escherichia coli*, a member of the heme−copper terminal oxidase superfamily, physiologically catalyzes reduction of O_2 by quinols and simultaneously translocates protons across the cytoplasmic membrane. The reaction of its ferric pulsed form with hydrogen peroxide was investigated with steady-state resonance Raman spectroscopy using a homemade microcirculating system. Three oxygen-isotope-sensitive Raman bands were observed at 805/*X*, 783/753, and (767)/730 cm^{-1} for intermediates derived from $H_2{}^{16}O_2/H_2{}^{18}O_2$. The experiments using $H_2{}^{16}O^{18}O$ yielded no new bands, indicating that all the bands arose from the Fe═O stretching ($\nu_{Fe=O}$) mode. Among them, the intensity of the 805/*X* cm^{-1} pair increased at higher pH, and the species giving rise to this band seemed to correspond to the P intermediate of bovine cytochrome *c* oxidase (CcO) on the basis of the reported fact that the P intermediate of cytochrome *bo* appeared prior to the formation of the F species at higher pH. For this intermediate, a Raman band assignable to the C−O stretching mode of a tyrosyl radical was deduced at 1489 cm^{-1} from difference spectra. This suggests that the P intermediate of cytochrome *bo* contains an Fe^{IV}═O heme and a tyrosyl radical like compound I of prostaglandin H synthase. The 783/753 cm^{-1} pair, which was dominant at neutral pH and close to the $\nu_{Fe=O}$ frequency of the oxoferryl intermediate of CcO, presumably arises from the F intermediate. On the contrary, the (767)/730 cm^{-1} species has no counterpart in CcO. Its presence may support the branched reaction scheme proposed previously for O_2 reduction by cytochrome *bo*.

Cytochrome *bo*-type ubiquinol oxidase from *Escherichia coli* is a member of the heme−copper terminal oxidase superfamily (see *1, 2* for reviews). It catalyzes the two-electron oxidation of ubiquinol-8 and the four-electron reduction of O_2, which are coupled with the vectorial transport of four protons across the cytoplasmic membrane. Unlike the aa_3-type cytochrome *c* oxidase (CcO),[1] cytochrome *bo* lacks the Cu_A site, while it contains three other redox-active metal centers in subunit I. In addition, cytochrome *bo* receives electrons from quinols, in place of ferrous cytochrome *c* in CcO. Despite such differences, close similarities in primary sequences (*3*) and X-ray structures (*4*−*7*) are found between subunits I, II, and III.

Spectroscopic properties of the intermediates of terminal oxidases generated during the reduction of O_2 to water have been extensively studied to understand the O_2 chemistry in biological systems. Visible absorption spectroscopy has proposed the following reaction scheme (*8*−*11*). The reaction of the reduced CcO with O_2 yields primarily an oxy species, which decays first into the P[2] species with a difference peak at 607 nm ("607-nm" species), then into the F[2] species with a major difference peak at 580 nm ("580-nm" species), and finally to the oxidized (O) species. The last two reduction steps are thought to be mainly coupled with vectorial proton pumping (*12, 13*), although recent results indicate that only three protons are involved in these steps but one in the reduction process of O (*14, 15*). The F species has been considered to have an oxyferryl heme (Fe^{IV}═O), whereas the structure of the P species has been under debate (*16, 17*). Although the visible absorption spectra reflect the redox changes of both hemes *a* and a_3, resonance Raman (RR) spectroscopy can bring about decisive information on the Fe(a_3)−oxygen moiety (see ref *18* for a review). The structures of heme a_3 in the oxy, P, F, and O states have been definitely determined to be the end-on dioxygen adduct with ν_{Fe-O_2} at 571 cm^{-1}, ironoxo form with $\nu_{Fe=O}$ at 804 cm^{-1}, ferryloxo form with $\nu_{Fe=O}$ at 785 cm^{-1}, and ferric hydroxy form with ν_{Fe-OH} at 450 cm^{-1} (*19*−*21*).

On the other hand, it has been demonstrated by time-resolved RR study that the reaction of the reduced cytochrome *bo* with O_2 involves intermediates similar to those

† This work was supported by a Grant-in-Aid for Scientific Research on Priority Areas (Molecular Biometallics) by the Ministry of Education, Science, Sports, and Culture, Japan (08249106 to T.K.). T.U. was supported by a fellowship from the Japan Society for Promotion of Science to Japanese young scientists.

* To whom correspondence should be addressed. Fax: +81-564-55-7340. Phone: +81-564-55-4639. E-mail: teizo@ims.ac.jp.

‡ Institute for Molecular Science, Okazaki National Research Institutes.

§ University of Tokyo.

[1] Abbreviations: CcO, cytochrome *c* oxidase; RR, resonance Raman; HRP, horseradish peroxidase; CCP, cytochrome *c* peroxidase; LPO, lactoperoxidase.

[2] The P and F intermediates have the oxidation states of the heme a_3/Cu_B moiety higher than the Fe^{3+}/Cu^{2+} state by 2 and 1 oxidative equiv, respectively, and correspond to the oxidation states of compounds I and II of a peroxidase, respectively.

10.1021/bi992538r CCC: $19.00 © 2000 American Chemical Society
Published on Web 05/09/2000

of CcO (*22*): the oxy species with ν_{Fe-O_2} at 568 cm^{-1} and the F species with $\nu_{Fe=O}$ at 788 cm^{-1}. However, the intermediate corresponding to the P species has not been clearly detected. Another approach for studying the reaction intermediates of cytochrome *bo* is to investigate the reaction of the oxidized enzyme with H_2O_2. Indeed, the structures of heme a_3 in the P and F intermediates of CcO in O_2 reduction are identical with those in the reaction of the oxidized CcO with H_2O_2 (*23*). Several groups also suggested that the reactions of the reduced CcO with O_2 and of the oxidized CcO with H_2O_2 share a common pathway after the formation of the P intermediate (*8*, *9*, *24*, *25*). Experimental conditions, including the concentrations of enzyme and H_2O_2, the pH, and the addition rate of H_2O_2, determine the relative populations of the P, F, and O species in the steady-state mixtures. In the case of CcO, the P species is predominant under the low concentration of H_2O_2 at pH 7.4 (but minor at pH <7.0), whereas the F species is dominant under high concentration of H_2O_2 at pH 9−10 (but P is dominant at pH 8)(*23*−*27*). It was demonstrated by taking advantage of these properties that the 607 nm species has an oxoheme (*28*) with the Fe=O stretching ($\nu_{Fe=O}$) mode at 804 cm^{-1} but not a peroxy heme [Fe−O−O (H)] which had been postulated before that time (*17*, *26*, *29*).

To explore the O_2 chemistry of quinol oxidases further in this study, we examined the reaction of the ferric pulsed cytochrome *bo* with H_2O_2 by steady-state RR spectroscopy using the microcirculating system (*30*) under different concentrations of H_2O_2 at various pHs. Three oxygen-isotope-sensitive Raman bands were found, and a possible branching of the reaction pathway will be discussed. In addition, a Raman band assignable to a neutral tyrosyl radical was derived digitally for the P intermediate from the double difference spectra of intermediates for the first time.

MATERIALS AND METHODS

Purification of Cytochrome bo. Cytochrome *bo* was purified from the *E. coli* GO103/pHN3795-1 (*cyo*$^+$ Δ*cyd*/*cyo*$^+$), as described previously (*22*, *31*). The enzyme was solubilized from the cytoplasmic membranes with sucrose monolaurate (Mitsubishi-Kagaku Foods) and purified by anion-exchange HPLC on DEAE-5PW (Tosoh). The purified enzyme was dissolved in 50 mM Tris-HCl (pH 7.4) containing 0.1% sucrose monolaurate and stored at −80 °C until the measurements. The data were acquired with the pulsed enzyme activated by procedures as described (*32*). The D_2O buffers were prepared in the same way as those of H_2O, and their pD values were adjusted according to the reading of a pH meter (pH*) the same as those for the H_2O solutions. A reduced form was prepared by adding a slight excess of freshly prepared dithionite solution into the degassed enzyme solution under an Ar atmosphere. A CO-bound form was prepared by incorporating CO gas into an airtight Raman cell containing the reduced form.

Resonance Raman Measurements. Resonance Raman spectra of the H_2O_2-treated cytochrome *bo* were measured under steady-state conditions using the microcirculating system (*30*). The total volume of sample circulated was ∼2.0 mL. Raman scattering was excited with the 406.7 and 413.1 nm lines from a Kr^+ ion laser (Spectra Physics, BeamLok 2060) with a power of 8−10 mW at the sample point, and scattered light was dispersed with a single polychromator (Ritsu Oyo Kogaku, DG-1000) equipped with a liquid N_2-cooled charge-coupled device (CCD) detector (PAR EG&G, CCD-1340/400-EB). Raman shifts were calibrated with ethanol and acetone in the flow cell as the second standards, which were calibrated with indene to an accuracy of ±1 cm^{-1} for intense isolated bands. All the Raman spectra presented are normalized by the intensity of the porphyrin ν_7 band at 677 cm^{-1}. A featureless fluorescence background was subtracted from each spectrum. The RR spectra of the reduced and CO-bound forms were measured with a quartz spinning cell (1600 rpm) with the 422.6 nm line from a diode laser (Hitachi Metals, ICD430). Raman shifts were calibrated with indene and CCl_4. All measurements were performed at room temperature. All the data analyses and graphic presentations were performed with Igor Pro (WaveMetrics).

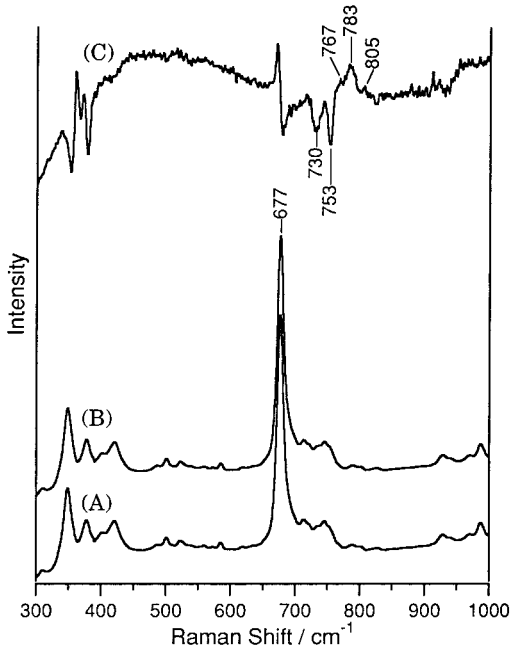

FIGURE 1: Resonance Raman spectra of reaction intermediates of ferric pulsed cytochrome *bo* with natural-abundance $H_2{}^{16}O_2$ (A) and $H_2{}^{18}O_2$ (B) in the steady state. Spectrum C represents the difference, spectrum A *minus* spectrum B. Experimental conditions: excitation wavelength, 413.1 nm; laser power at the sample point, 8−10 mW; room temperature; sample concentration, 25 μM; $[H_2O_2] = 2$ mM. After initiation of the reaction, 50 mM H_2O_2 stock solution was continuously added to the circulating enzyme solution at the rate of 0.55 nmol of H_2O_2 (nmol of enzyme)$^{-1}$ min^{-1}. Accumulation time was 2 × 30 min. Intensities of Raman spectra are normalized with respect to the porphyrin ν_7 band at 677 cm^{-1}. The featureless fluorescence background was subtracted using the polynomial function, and the baseline was made flat.

Materials. $H_2{}^{16}O_2$ [30% (w/v), Wako Pure Chemicals] was used as purchased. $H_2{}^{18}O_2$ was prepared from $^{18}O_2$ as described by Sawaki and Foote (*33*), although a part of $H_2{}^{18}O_2$ was a gift from Dr. T. Matsui of the Institute for Molecular Science and Dr. M. Tanaka of Kyoto University. $H_2{}^{16}O^{18}O$ was a gift from E. H. Appelman of Argonne National Laboratory. The concentration of H_2O_2 was determined by iodimetric assay (*34*).

RESULTS

RR Spectra in the Reaction of Cytochrome bo with H_2O_2. Figure 1 shows the 413.1 nm excited RR spectra in the 300−

1000 cm^{-1} region of the ferric pulsed cytochrome *bo* reacted with $H_2{}^{16}O_2$ (A) and $H_2{}^{18}O_2$ (B) at pH 7.4. The difference spectrum (C) exhibited three oxygen-isotope-sensitive Raman bands at 805/*X*, 783/753, and *Y*(767)/730 cm^{-1} for $H_2{}^{16}O_2$/$H_2{}^{18}O_2$ derivatives. The band positions, *X* and *Y*, could not be determined unequivocally from the observed spectra due to overlapping of the bands, although *Y* was deduced with the help of simulation as described later. The experiment with $H_2{}^{16}O^{18}O$ did not give rise to a new peak (data not shown). Therefore, all the oxygen-isotope-sensitive bands observed in Figure 1 are assignable to the Fe═O stretching ($\nu_{Fe=O}$) modes, but not to the O−O stretching mode.

The oxygen-isotope-sensitive band at 783/753 cm^{-1} is most intense and is almost identical to that obtained in the reaction of the reduced cytochrome *bo* with $^{16}O_2/^{18}O_2$ using the artificial cardiovascular system (*22*). The corresponding band was also observed at 785/750 cm^{-1} in the catalytic cycle of bovine CcO and assigned to the Fe^{IV}═O mode of the F intermediate (*19*−*21*). The $^{16}O/^{18}O$ isotope shift of 30 cm^{-1} in this spectrum is close to that expected for an isolated Fe═O stretch at 783 cm^{-1}. Although the 805/*X* cm^{-1} band was not clearly identified in our previous time-resolved RR study for the reaction of the reduced cytochrome *bo* with O_2 (*22*), the reaction with H_2O_2 made the presence of this band clear. This band is similar to the 804 cm^{-1} band of the 607 nm species of bovine CcO, which has been assigned to the $\nu_{Fe=O}$ mode of the P intermediate (*19*, *25*, *28*). The lowest frequency band at (767)/730 cm^{-1} was detected as the $\nu_{Fe=O}$ band of reaction intermediates of terminal oxidases for the first time, although a similar band was observed at 767/727 (or 753/725) cm^{-1} for compound ES of cytochrome *c* peroxidase (CCP) (*35*, *36*) and at 745/712 cm^{-1} for compound II of lactoperoxidase (LPO) (*36*). Lowering of the $\nu_{Fe=O}$ frequency can be attributed to a strong hydrogen bond from distal amino acid residue(s) to the oxoferryl oxygen, and the trans effect of the proximal ligand (*36*−*38*).

The ferric hydroxy intermediate with the Fe−OH stretch (ν_{Fe-OH}) at 450 cm^{-1} as observed for the reaction of bovine CcO with O_2 (*19*, *20*) was not detected in this reaction. Probably, fast exchange of a hydroxy group with solvent water molecules makes it difficult to identify an oxygen-isotope-sensitive band similar to the case of the reaction of the oxidized CcO with H_2O_2.

pH-Dependence of Difference RR Spectra. Figure 2 illustrates the pH-dependence of the $H_2{}^{16}O_2/H_2{}^{18}O_2$ difference Raman spectra for the reaction intermediates of the ferric pulsed cytochrome *bo* with hydrogen peroxide. The relative intensity of the positive band at 808 cm^{-1} to that at 783 cm^{-1} increased at alkaline conditions, and the presence of the 808 cm^{-1} band became undoubted. However, the Raman intensities of the oxygen-isotope-sensitive bands as a whole were getting weaker as the pH increased. This indicates that the amount of a ferric form increases in the steady state at higher pH with the expense of the reaction intermediates or that the exchange rate of the iron-bound oxygen atom with bulk water ($H_2{}^{16}O$) increases after the formation of the Fe═^{18}O species. The latter was encountered in compound II of HRP (*37*) and compound ES of CCP (*35*) at neutral pH but not at alkaline pH. It was considered that a hydrogen bond between the oxygen atom and the surrounding amino acid residue(s), probably distal histidine, is indispensable to perform the exchange reaction.

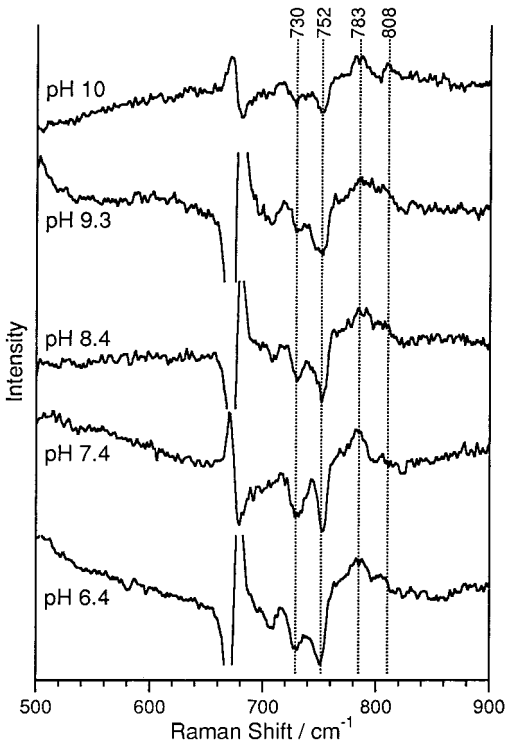

FIGURE 2: pH-Dependence of the oxygen-isotope difference spectra between intermediates in the reaction of ferric pulsed cytochrome *bo* with $H_2{}^{16}O_2$ and $H_2{}^{18}O_2$. The experimental conditions were the same as those in Figure 1. Different buffers were used at individual pH regions: sodium phosphate for pH 6.4 and 7.4; Tris-HCl for pH 8.4; sodium borate for pH 9.3 and 10.0.

The presence of a hydrogen bond in the 805 cm^{-1} species was suggested by its pH-dependent frequency shift: from 805 cm^{-1} at pH 7.4 to 808 cm^{-1} at pH 10.0. However, the broadening of the bands at 783 and 805 cm^{-1} around pH 8.4−9.3 inhibited separation of the two bands and thus determination of the pK_a value of the transition. In the 805 cm^{-1} species of cytochrome *bo* at low pH, a distal amino acid residue may also interact with the ferryloxo oxygen as in HRP-compound II, which makes the $\nu_{Fe=O}$ frequency lower, but this interaction is disrupted by deprotonation of the distal group in the pH region higher than its pK_a value, and as a result, the 805 cm^{-1} band shifts to a high frequency. It is possible that deprotonation of the distal residue may induce a tertiary structure change of the protein, which distorts the Fe−His bond in the proximal side as seen for HRP (*39*) and induces some trans effect on the $\nu_{Fe=O}$ mode. However, the pH-dependent behavior of the Fe−His stretching (ν_{Fe-His}) frequency eliminates this possibility as mentioned later.

Effect of D_2O Substitution. If the ferryloxo oxygen is hydrogen bonded to the distal residue; the $\nu_{Fe=O}$ frequency would be changed upon H/D exchange. Furthermore, the lifetime of the P intermediate might be significantly longer in D_2O than in H_2O as for bovine CcO (*19*). Accordingly, the effect of D_2O substitution on the difference spectra was investigated. Figure 3 shows the $H_2{}^{16}O_2/H_2{}^{18}O_2$ difference RR spectra of cytochrome *bo* in the steady state at pH* 7.1 (A), 8.3 (B), and 9.5 (C) in D_2O buffer. The three oxygen-isotope-sensitive bands observed for the H_2O solution at pH 7.4 (Figure 1C) are reduced to one in D_2O at pH* 7.1 (A), and the peak position shifts from 783/753 cm^{-1} (H_2O) to 789/756 cm^{-1} (D_2O). This indicates that the rates of

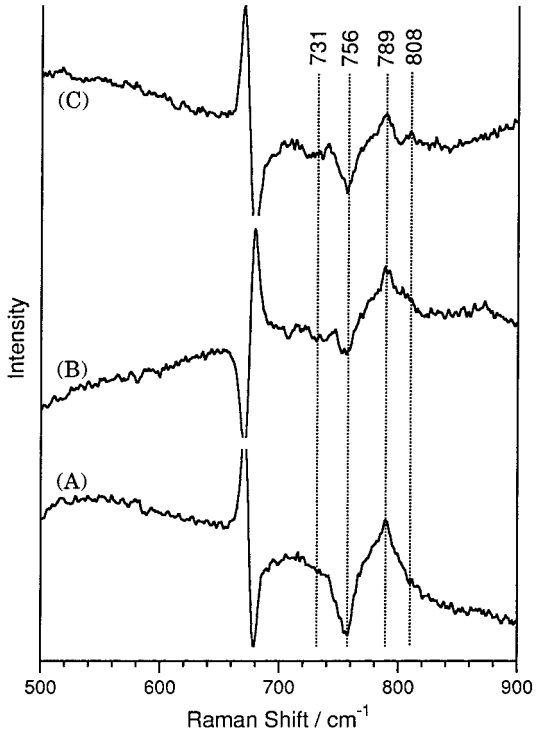

FIGURE 3: pH*-Dependence of the oxygen-isotope difference spectra between intermediates in the reaction of ferric pulsed cytochrome *bo* with $H_2{}^{16}O_2$ and $H_2{}^{18}O_2$: (A) pH* 7.1; (B) pH* 8.3; (C) pH* 9.5. The experimental conditions were the same as those in Figure 1.

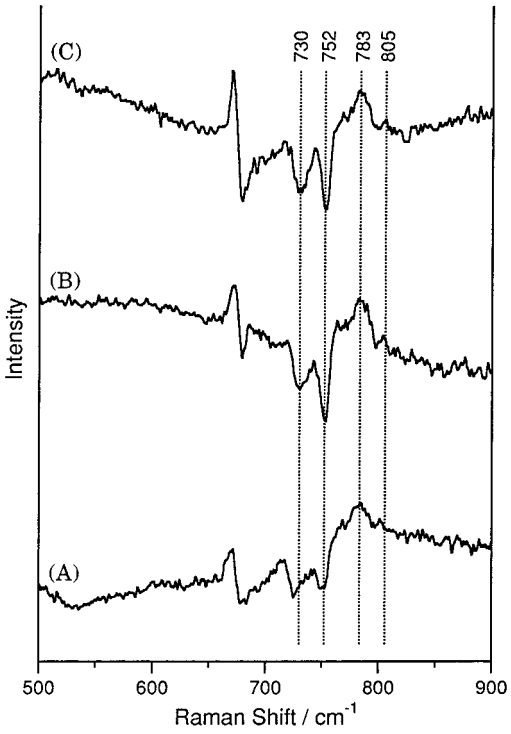

FIGURE 4: H_2O_2 concentration dependence of the oxygen-isotope difference spectra between intermediates in the reaction of ferric pulsed cytochrome *bo* with $H_2{}^{16}O_2$ and $H_2{}^{18}O_2$ at pH 7.4: (A) $[H_2O_2] = 0.1$ mM; (B) $[H_2O_2] = 0.5$ mM; (C) $[H_2O_2] = 2$ mM. The experimental conditions were the same as those in Figure 1.

elementary steps in the catalytic cycle are affected by H/D exchange and, as a result, the 789/756 cm^{-1} intermediate was accumulated in the steady state in D_2O.

The most intense 783 cm^{-1} band in H_2O at pH 7.4 is upshifted to 789 cm^{-1} upon H/D exchange (Figures 1 and 3). The amount of upshift on the H/D exchange in cytochrome *bo* (6 cm^{-1}) is larger than that of CcO (2 cm^{-1}) (*19*, *28*). The high-frequency shift upon D_2O substitution suggests the presence of a hydrogen bond to the iron-bound oxygen as in peroxidases (*35*, *37*, *40*). However, the 783 cm^{-1} band exhibited little pH-dependent frequency shift (Figure 2). The absence of pH-sensitivity and the presence of H_2O/D_2O frequency difference imply that the hydrogen bond is present at pH 7−9 and that the pK_a value of this species is above 10. Then, the pK_a values of the ionizing residues differ with intermediates. There is a possibility that the hydrogen bond partner of the ferryloxo oxygen in the 783 cm^{-1} species is different from that in the 805 cm^{-1} species or the pK_a value of the particular residue changes between the P and F intermediates. Anyhow, this suggests that some significant structural change takes place at the distal side between the P and F intermediates. Despite the presence of the hydrogen bond, the exchange of an iron-bound oxygen atom with bulk water is repressed in the 783 cm^{-1} intermediate, which differs from compound II of HRP under neutral conditions (*37*). The repression of oxygen exchange is presumably caused by the absence of water at the distal pocket.

At higher pH*, especially pH* 9.5, weak positive and negative bands appeared at 808 and ∼731 cm^{-1}, which correspond to the bands observed at 808 and 730 cm^{-1} in H_2O, respectively (Figures 2 and 3). These two bands scarcely shifted on H/D exchange, suggesting that the distal amino acid residues do not make a hydrogen bond with the ferryloxo oxygen of the 808 and (767)/730 cm^{-1} species.

H_2O_2 Concentration Dependence of Difference RR Spectra. Figure 4 displays the H_2O_2 concentration dependence of the $H_2{}^{16}O_2/H_2{}^{18}O_2$ difference spectra at pH 7.4 in H_2O. The peak positions and relative intensities in the difference spectra showed little change over the H_2O_2 concentration range from 0.1 to 2.0 mM,[3] except for a slight low-frequency shift of the negative ∼730 cm^{-1} band at $[H_2O_2] = 0.1$ mM. The insensitivity to the H_2O_2 concentration was also encountered at pH 10 in H_2O, and at pH* 7.3 and 9.5 in D_2O (data not shown). These indicate that the binding of H_2O_2 to the ferric cytochrome *bo* is not the rate-determining step of the entire reaction or, alternatively, is too slow to be influenced by this change of the H_2O_2 concentration.

Heme Environmental Structures under Various pHs. To examine the pH dependency of amino acid residues in the heme proximity, the RR spectra of the dithionite-reduced and CO-adduct forms of cytochrome *bo* were measured at various pHs. The RR spectra of the reduced form in the low-frequency region (170−400 cm^{-1}) are presented in Figure 5, in which the spectrum at pH 7.4 is in agreement with that reported (*41*). The Raman band at 208 cm^{-1}, which completely disappeared upon addition of CO (bottom), was assigned to the ν_{Fe-His} mode of heme *o* (*41*). The center frequency and width of this band were insensitive to pH over the 6−10 range. This suggests that the Fe−His bond in the

[3] It is difficult to measure RR spectra for the reaction of cytochrome *bo* with H_2O_2 more concentrated than $[H_2O_2] = 2$ mM due to strong fluorescence background originating from rapid degradation of heme *o*.

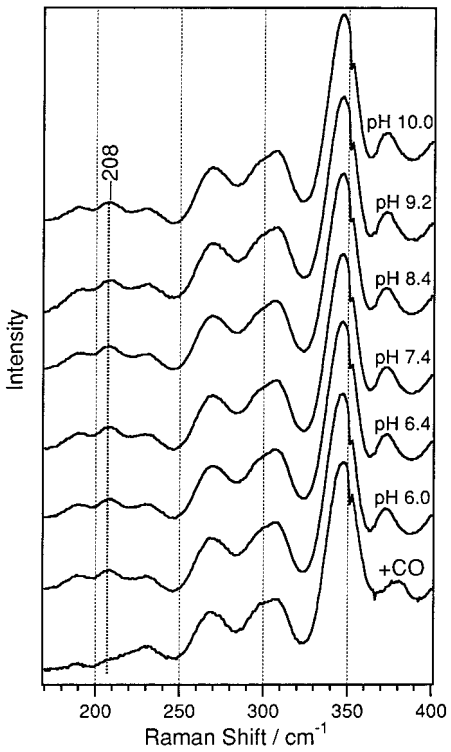

FIGURE 5: pH-Dependence of resonance Raman spectra of the reduced form of cytochrome *bo* in the low-frequency region. Experimental conditions: excitation wavelength, 422.6 nm; laser power at the sample point, 3.4 mW; room temperature; sample concentration, 25 μM. The sample solution was placed in an airtight Raman spinning cell (1600 rpm).

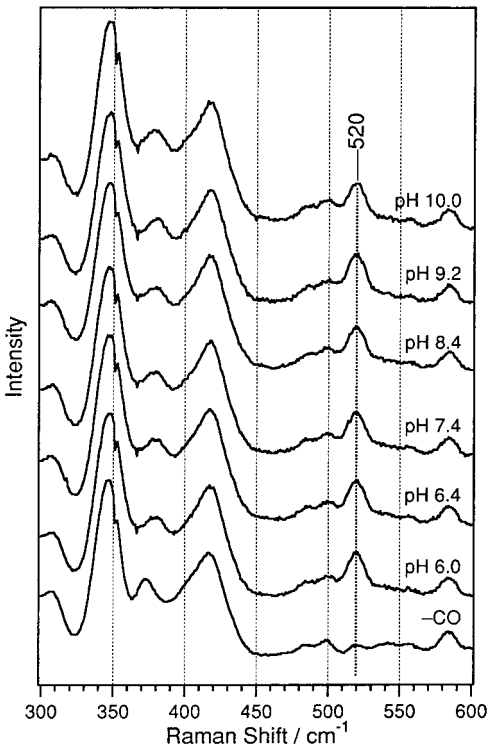

FIGURE 6: pH-Dependence of resonance Raman spectra of the CO-bound form of cytochrome *bo* in the low-frequency region. Experimental conditions were the same as those in Figure 5 except that the laser power at the sample point was 0.3 mW.

proximal side was not altered by pH change and thus is not expected to induce the trans effect on the $\nu_{Fe=O}$ mode.

Figure 6 shows the RR spectra in the 300−600 cm^{-1} region of the ferrous CO form. The band at 520 cm^{-1} was downshifted by 12 cm^{-1} with $C^{18}O$ and disappeared upon increase of laser power. Therefore, the 520 cm^{-1} band is assigned to the Fe−CO stretch. The band position is slightly shifted (by 3−4 cm^{-1}) from those reported (*42*, *43*). If the heme environments change with pH, the Fe−CO stretching frequency is expected to shift as demonstrated for HRP-CO (*44*) and MbCO (*45*). However, neither the position nor the width of the Fe−CO stretching band exhibited prominent pH-dependence. In fact, the C−O stretching is also reported to be pH-insensitive between pH 7 and 10 (*46*). The results shown in Figures 5 and 6 demonstrate that the environmental structure of heme *o* is quite insensitive to pH in the pH 6−10 range, suggesting that the shift of the $\nu_{Fe=O}$ frequencies and the alteration of the relative intensities (Figures 2 and 3) are not always due to the conformational change around heme *o*. These results are in contrast with the pH-dependent conformational change at the heme−copper binuclear center in the reduced CO-bound form of CcO (*47*).

RR Spectra in the High-Frequency Region. RR spectra in the high-frequency region of the ferric pulsed (A) and H_2O_2-treated cytochrome *bo* (B) at pH 10.0, $[H_2O_2] = 0.5$ mM, excited at 406.7 nm and their difference spectra (C) are depicted in Figure 7, where the difference, H_2O_2-treated *minus* ferric pulsed forms at pH* 7.1, is also included for later discussion. The RR spectral features of the ferric cytochrome *bo* are in agreement with those reported (*42*, *43*). The ν_4 band appears at 1369 cm^{-1}. The ν_3 bands of hemes *b* and *o* were observed at 1501 and 1476 cm^{-1} in accord with the six-coordinate ferric low-spin and high-spin states, respectively. Addition of H_2O_2 apparently causes little spectral change, but the difference spectrum (C) revealed that the intensities of the bands at 1503, 1588, and 1640 cm^{-1} increased and those at 1476, 1566, and 1619 cm^{-1} decreased. The intensity decreases of the ν_2 (1571 cm^{-1}) and ν_3 (1476 cm^{-1}) bands, which are the well-established coordination- and spin-state marker bands, indicate that the six-coordinated high-spin heme *o* reacts with H_2O_2 and changes its coordination- and spin-states (*42*).

DISCUSSION

Assignments of Oxygen-Isotope-Sensitive RR Bands. In the steady-state experiments for the reaction of the ferric pulsed cytochrome *bo* with $H_2{}^{16}O_2/H_2{}^{18}O_2$ using the microcirculating system, three oxygen-isotope-sensitive RR bands were observed at 805/*X*, 783/753, and *Y*(767)/730 cm^{-1} in the $\nu_{Fe=O}$ region (Figure 1). The band at 783/753 cm^{-1} is almost identical to that observed for the reaction of this enzyme with O_2 (*22*). Although it was not distinguished whether the broad band around 785 cm^{-1} for the O_2 reaction was composed of one or two bands, the band was separated in this study into two bands, 805/*X* and 783/753 cm^{-1}, by using H_2O_2 as an oxidant. These two bands were common among the intermediates observed in dioxygen reduction by CcO (*19*−*21*, *23*, *28*). It is noted, however, that the lowest frequency band at *Y*(767)/730 cm^{-1} is newly observed in the reaction of terminal oxidases. The band position of *Y* was determined through a simulation method, in which a Lorentzian band was assumed at various frequencies for a $H_2{}^{16}O_2$ derivative with fixed frequencies for other bands, and difference spectra between the $H_2{}^{16}O_2$ and $H_2{}^{18}O_2$ derivatives

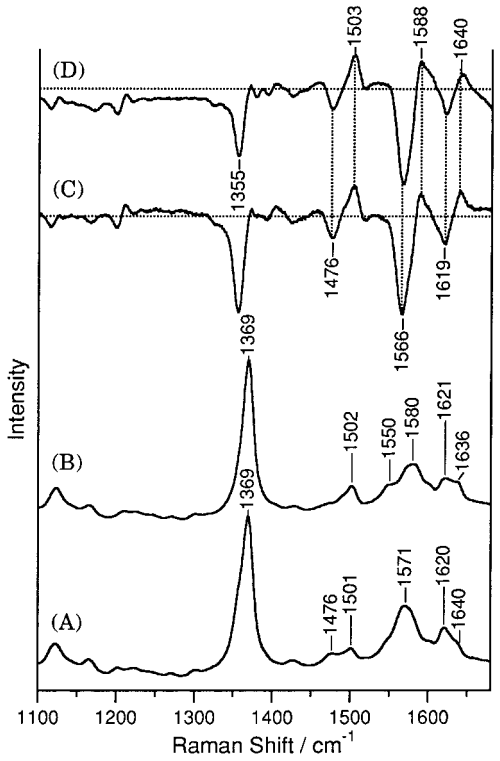

FIGURE 7: Resonance Raman spectra in the high-frequency region of the ferric pulsed (A) and H_2O_2-treated (B) forms of cytochrome *bo* at pH 10.0, $[H_2O_2] = 0.5$ mM. Spectrum C is a difference, spectrum B *minus* spectrum A. Spectrum D is a difference, the H_2O_2-treated *minus* ferric pulsed forms at pH* 7.1, $[H_2O_2] = 2$ mM. The excitation wavelength is 406.7 nm, and the laser power is 6 mW at the sample point. Other experimental conditions were the same as those in Figure 1.

were calculated until the calculated pattern reproduces the observed one. The ν_{Fe-OH} band at 450 cm^{-1} derived from the hydroxy intermediate and the 350 cm^{-1} band of the intermediates were also weakly observed, although the peak positions could not be identified.[4]

To date, there have been many studies to propose the reaction mechanism of dioxygen reduction by cytochrome *bo* on the basis of time-resolved visible absorption (*11*, *32*, *48*, *49*), RR (*22*, *42*), and MCD (*50*) spectroscopic studies. Time-resolved absorption spectroscopy found a characteristic intermediate with an absorption maximum at 557 nm under micromolar concentrations of H_2O_2 at neutral pH (*32*, *48*). This species was shown by MCD spectra to contain an oxyferryl heme but not a porphyrin π-cation radical (*50*). In the present RR spectra, the 783 cm^{-1} band is dominant under the conditions in which the 557 nm absorption band was seen; $[H_2O_2] = 2$ mM at pH 7.4 (Figure 1). The size of an ^{18}O-isotope frequency shift (30 cm^{-1}) is reasonable to assign the 783 cm^{-1} band to the Fe═O stretch. Furthermore, its frequency is close to the $\nu_{Fe=O}$ frequency of the oxyferryl species of CcO (785/750 cm^{-1}) (*19*−*21*). Accordingly, it is reasonable to assign the 783/753 cm^{-1} band of cytochrome *bo* to an oxyferryl intermediate.

On the other hand, an additional intermediate with the absorption maximum at 582 nm was observed prior to the oxyferryl intermediate under high concentrations of H_2O_2 and alkaline pH, and this species has been assigned to the P intermediate (*17*, *49*). Among the three $\nu_{Fe=O}$ Raman bands, a slight increase in intensity was noticed for the 808 cm^{-1} band at pH 10 (Figure 2). This frequency is close to the $\nu_{Fe=O}$ frequency of the P species of bovine CcO (804 cm^{-1}) (*19*, *28*). Accordingly, it is likely that the 808 cm^{-1} band arises from the P species of cytochrome *bo*. Although we tried to excite Raman scattering in the vicinity of the absorption maximum of the P species (582 nm), strong fluorescence made it impossible to get well-defined Raman spectra.

Newly Observed Intermediate. The assignment of the lowest frequency species with a band at (767)/730 cm^{-1} remains to be determined. This frequency is quite lower than general $\nu_{Fe=O}$ frequencies with two noticeable exceptions: compound ES of CCP (753 or 767 cm^{-1}) (*35*, *36*) and compound II of LPO (745 cm^{-1}) (*36*). The low $\nu_{Fe=O}$ frequency can be attributed to the trans effect by proximal ligand (*51*), strong hydrogen bonding to the iron-bound oxygen (*36*, *37*), and the electronic character of the porphyrin (*52*).

The $\nu_{Fe=O}$ frequencies of the five-coordinated oxyferryl model compounds appear at ∼840−850 cm^{-1} in the absence of a strong ligand (*38*). Addition of imidazoles to these compounds as a sixth ligand resulted in a decrease in the $\nu_{Fe=O}$ frequency by 20−30 cm^{-1} (*53*). Furthermore, it was shown that there is a significant positive correlation between the $\nu_{Fe=O}$ frequencies of compounds II of peroxidases and their ν_{Fe-His} frequencies of the ferrous five-coordinated form (*51*). These studies concluded that the ligation of the strong ligand to the heme reduces the electron donation from the oxo atom to the heme iron, resulting in a decrease in the $\nu_{Fe=O}$ frequencies of the oxyferryl compounds. However, the ν_{Fe-His} frequency of the ferrous cytochrome *bo* (208 cm^{-1} in Figure 5) is significantly lower than those of peroxidases, and even lower than those of oxygen transport proteins (∼220 cm^{-1} for deoxyMb and deoxyHb) (*54*). This suggests that the trans effect is not the main factor for the low $\nu_{Fe=O}$ frequency of the 767/730 cm^{-1} species.

A hydrogen bond from the surrounding amino acid residue to the iron-bound oxygen also causes a decrease in the $\nu_{Fe=O}$ frequency of oxoferryl compounds (*35*−*37*, *40*). However, the (767)/730 cm^{-1} band showed little frequency shift upon D_2O substitution (Figures 1 and 3), which indicates that the hydrogen bond in this species is quite weak. Furthermore, the Fe═^{18}O bond of the (767)/730 cm^{-1} species of cytochrome *bo* can be observed sharply even in $H_2{}^{16}O$ (Figures 1 and 2), in contrast with the case of compound II of HRP (*37*), indicating negligible exchange of the Fe═O oxygen with bulk water and thus that the hydrogen bond in this species is not so strong. Therefore, it is difficult to account for the lower $\nu_{Fe=O}$ frequency of the oxyferryl cytochrome *bo* by the hydrogen bonding effect.

The electron-donating/withdrawing character of the porphyrin macrocycle can also affect the $\nu_{Fe=O}$ frequency (*52*). When a porphyrin ring is electron-deficient by the presence of electron-withdrawing side chains, the π-donor strength of the ferryl oxygen atom increases, which would lead to the stronger Fe═O bond and thus higher $\nu_{Fe=O}$ frequency (*38*, *52*). The active site modeling of cytochrome *bo* (*55*, *56*) suggested that Asp407 approaches heme *o* and donates electrons. If this is the case, the $\nu_{Fe=O}$ frequency would

[4] Some positive and negative bands appeared around 350 cm^{-1} on the difference spectrum (Figure 1). However, a lack of reproducibility of these bands does not allow us to note that they are oxygen-isotope-sensitive bands. Probably, a slight distortion on subtracting the fluorescence background may cause poor reproducibility.

Scheme 1

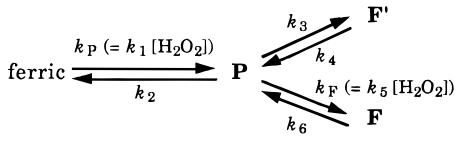

decrease, and this newly observed intermediate implies the presence of unique aspects in the structure of the heme pocket of the (767)/730 cm^{-1} species of cytochrome *bo*.

pH and H_2O_2 Concentration Dependence of RR Difference Spectra. Since the present study is based on the steady-state measurements, it is difficult to determine the oxidation state and the order of appearance of each intermediate in the reaction. However, this can be discussed on the basis of the pH and H_2O_2 concentration dependence of the RR difference spectra. Current knowledge about the reaction intermediates of cytochrome *bo* obtained from time-resolved absorption spectroscopy includes that an intermediate with an absorption maximum (λ_{max}) at 557 nm appears under low concentration of H_2O_2 at neutral pH (*32*, *48*) but that with λ_{max} at 582 nm appears prior to the 557 nm species at higher concentration of H_2O_2 at alkaline pH (*17*, *49*). Accordingly, the 582 and 557 nm absorbing species are considered to correspond to the P and F intermediates of cytochrome *bo*.

The branched reaction scheme (Scheme 1) was proposed for the reaction of cytochrome *bo* with H_2O_2 from the transient optical absorption measurements upon rapid mixing (*49*). According to the scheme, the P species was initially formed from the ferric cytochrome *bo* in a bimolecular reaction with H_2O_2. Subsequent reduction by a second equivalent of H_2O_2 or by a unknown reductant converts the P species to an oxoferryl species, F or F′. The relative contribution of the F′ to F species mainly depends on the concentration of H_2O_2 used. Only the F′ species was observed under the low concentration of H_2O_2 at neutral pH (*17*, *32*, *49*). This suggests that the slow bimolecular reaction generating the P species followed by a rapid reduction to the F′ species prevents the accumulation of the P species ($k_P \ll k_3$). On the other hand, both the P and F species were observed under high concentrations of H_2O_2 at higher pH (*17*, *49*). This indicates that the acceleration of the formation rate of the P species makes it comparable to the formation rate of the F species ($k_P \sim k_F$). The present experimental conditions are close to those of the low H_2O_2 concentration in the absorption experiments. Therefore, it is expected that the difference RR spectra at neutral pH (Figure 1) may predominantly provide a band from the F′ species. This coincides with the assignment of the band at 783 cm^{-1} to the oxoferryl species (F′) as described above. On the other hand, the RR band at 805 cm^{-1}, whose intensity was increased at alkaline conditions (Figure 2), is compatible to arise from the P species. It is plausible that the ascent in pH or H_2O_2 concentration accelerates the formation of the P species, resulting in its accumulation if the decomposition rate remains unchanged.

Instead, a decrease in the decomposition rate of the P to F′ species (k_3) can also increase the population of the P species, if k_P remains unchanged. If both k_P and k_3 decrease, the lifetime of the F′ species may also be prolonged and the F′ species would be accumulated in the steady-state. However, the weaker intensities of all the $\nu_{Fe=O}$ bands at alkaline conditions (Figure 2) indicate that the lifetimes of both the P and F′ species are reduced at alkaline conditions against the expectation.

Mechanism of Generation of P Species. As demonstrated by the pH-dependence of the Fe−His and Fe−CO stretching modes (Figures 5 and 6), the heme *o* pocket structure was scarcely altered even at alkaline conditions. Therefore, the pH-dependence of the formation rate of the P species (k_P) would not be caused by a conformational change at the active site of cytochrome *bo*. This indicates that deprotonation of amino acid residues is involved in the process of the formation of the P species. Recent studies in the reaction of the fully reduced bovine CcO with O_2 postulated the transient generation of a tyrosyl radical in the P species at the active site (*57*). In this model, the formation of the P species is accompanied by generation of a neutral radical of Tyr244, which is derived by hydrogen atom transfer from Tyr244 to the iron-bound oxygen atom to promote O−O bond cleavage (*58*). When the P species is reduced to the F species, the Tyr244 neutral radical is converted to tyrosinate. The presence of tyrosine radical, which was confirmed by spectral changes due to deuteration of tyrosine, was also noted from EPR spectroscopy for the reaction of oxidized CcO with H_2O_2 (*59*).

Generation of the tyrosine radical is considered to be the unique character of Tyr244, which was revealed to be covalently bound to a Cu_B-coordinated His240 in the case of CcO by the recent X-ray crystallographic studies (*60*, *61*). Tyr244 of bovine CcO (Tyr280 in *Paracoccus denitrificans*; Tyr288 in *E. coli*) has been shown to be connected to the adjacent His240 (His276 in *P. denitrificans*; His284 in *E. coli*), which is one of the ligands of Cu_B, through a covalent bond in the fully oxidized, reduced, and CO-bound forms. This covalent linkage is expected to reduce the pK_a of the hydroxyl group of the tyrosine. Then, a significant amount of Tyr244 may be in a deprotonated form at neutral pH. Furthermore, the hydroxyl group of Tyr244 is located close to the iron-coordinated ligand enough to make a hydrogen bond with the ligand (*60*, *61*). These peculiar properties make it likely that Tyr244 serves as a general acid−base catalyst in the formation of the P species, similar to the distal histidine in most peroxidases.

Although the high-resolution crystal structure of cytochrome *bo* has not been resolved yet (*6*), the structural similarities and a number of physicochemical studies have led us to assume that the active site structure of cytochrome *bo* is very close to those of CcO except for the lack of Cu_A (*1*−*7*). On the basis of the pH-dependence of the difference RR spectra for the reaction of the ferric pulsed cytochrome *bo* with H_2O_2 shown in Figure 2, the formation mechanism of the P species in cytochrome *bo* can be speculated in analogy to that of HRP as illustrated in Scheme 2.

In the first step, a protein base-catalyst abstracts a proton from H_2O_2 (i). In most peroxidases, the distal histidine acts as the base-catalyst to accept a proton from H_2O_2 to form a putative hydroperoxo intermediate, Fe−O−OH (A in Scheme 2). The hydroperoxo intermediate is quite unstable, and the O−O bond is immediately cleaved heterolytically with the support of a hydrogen bond between the distal histidine and the iron-bound hydroperoxo in the case of peroxidases. Finally, the distal histidine provides a proton to the leaving hydroxide anion as a general acid, in turn, to produce a water

Scheme 2

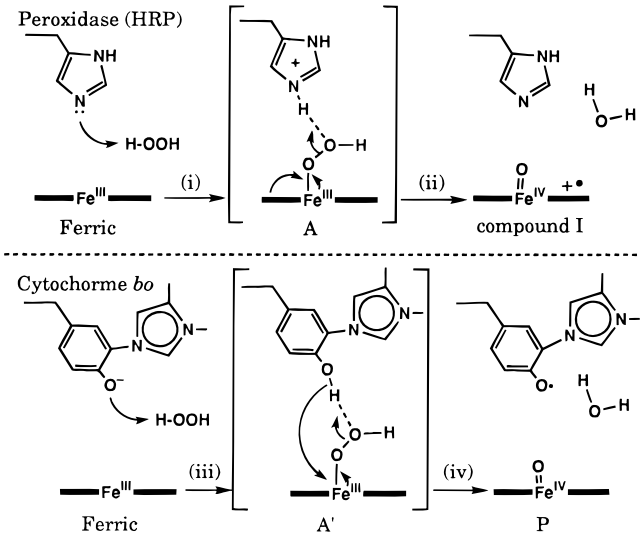

molecule and a stable high-valent intermediate accompanied by the oxidation of the porphyrin macrocycle [(ii) in Scheme 2]. The intermediate thus formed is an Fe^{IV}=O porphyrin π-cation radical called compound I.

In the case of cytochrome *bo*, on the other hand, Tyr288 is postulated to play a general acid−base catalyst similar to the distal His of HRP. First, deprotonated Tyr288 of the oxidized enzyme abstracts a proton from H_2O_2 [(iii) in Scheme 2]. Next, the protonated Tyr288, which has a lower pK_a value due to the covalent linkage to the side chain of His284, acts as a proton donor (general acid) and facilitates the scission of the O−O bond heterolytically to produce a water molecule and a high-valent iron intermediate [(iv) in Scheme 2]. For cytochrome *bo*, the absorption spectra in the Soret and visible regions exclude the formation of a porphyrin π-cation radical (*17, 32, 48*−*50*). Presumably, the tyrosinate ($Tyr288^-$) adjacent to the iron-bound ligand serving as an electron donor immediately becomes a neutral tyrosyl radical, yielding the P species (Fe^{IV}=O, tyrosine radical). Finally, reduction of the tyrosyl radical and protonation to it generate the F species (Fe^{IV}=O, ordinary tyrosine). This tyrosine may form a hydrogen bond with the oxoferryl oxygen. It has not been established that a tyrosine residue plays a role as a general acid−base catalyst. However, it is not only histidine that acts as a general acid−base catalyst in biological systems. In chloroperoxidase from *Caldariomyces fumago*, Glu186 is located at the position corresponding to the distal histidine of HRP and plays a role as a general acid−base catalyst (*62*). This indicates a possibility that a tyrosine acts as an acid−base catalyst for the peroxidase reaction if it is located in a proper position and has a suitable pK_a value.

For photosystem II, the mechanism of tyrosyl radical formation has been investigated in detail (*64, 65*), and the role of the tyrosyl radical as an acceptor of water protons to form an O−O bond has been proposed (*66*). Diner et al. (*67*) noted that the oxidation and deprotonation of Y_Z is the primary process which occurred through proton abstraction by a nearby base, followed by electron transfer. The oxidation rate of Y_Z[5] is larger at higher pH, and the pH-dependence is attributed to an increased population of tyrosinate (*68*). If this idea is applicable to cytochrome *bo*, the increase in pH leads to acceleration in the generation of a tyrosyl radical ($Tyr288^•$) and thus to an increase in the formation rate of the P species. This model coincides with the present assignment of the 805 cm^{-1} species to the P species, which has been observed clearly under alkaline conditions. In fact, a tyrosyl radical is found for compound I of prostagrandin H synthase (*63*).

The deuterium isotope effect of the RR spectra in the reaction of cytochrome *bo* with H_2O_2 can also be explained by Scheme 2, including the tyrosyl radical in the P species. Scheme 2 also shows that the deuterium transfer process participates in both (iii) and (iv), which retards the formation of the P species in comparison with the hydrogen case. Indeed, replacement of H_2O with D_2O lowers the rate of the oxidation of Y_Z in the case of the Mn-depleted photosystem II (*67*). Therefore, the deuterium isotope effect is expected to be opposite to that of the pH ascent, which suggests that the D_2O substitution shortens the lifetime of the P species and buries its RR band in the steady-state spectra. This agrees with the observed RR difference spectra of cytochrome *bo* obtained in D_2O (Figure 3), in which oxygen-isotope-sensitive bands other than the 789 cm^{-1} band were smeared. The oxidation rate of Y_Z in the Mn-depleted photosystem II becomes insensitive to deuterium substitution at higher pD (*67*). In accord, the difference RR spectra in D_2O become similar to those in H_2O at alkaline conditions (Figures 2 and 3).

RR Spectra of the Tyrosyl Radical. The assumption of the involvement of the tyrosyl radical in the P species of cytochrome *bo* can qualitatively account for the influence of pH change and D_2O substitution on the difference RR spectra of the steady-state mixture of intermediates in the reaction with H_2O_2. Recently, the ESR spin-trapping technique succeeded in detecting a protein radical in the reaction of CcO with H_2O_2 (*69*). To identify the involvement of the active-site tyrosyl radical in the intermediate of the peroxide reaction, we analyzed further the RR spectra in the high-frequency region.

Since the contribution of the 808 cm^{-1} species, which has been assigned to the P species in this study, is large at higher pH (Figure 2), the Raman band of the tyrosyl radical, if present, is expected to appear under such conditions. It is known that the absorption maximum of a tyrosyl radical lies around 408−410 nm (*70, 71*) and that the C−O stretching mode of a phenoxy radical is observable around 1500 cm^{-1} by infrared and RR spectroscopies (*71*−*74*). As expected, spectrum C in Figure 7 displays a positive intense band at 1503 cm^{-1}. To confirm whether this band is derived from the tyrosyl radical in the P species, we examined other differences between spectra obtained under the conditions where the 808 cm^{-1} band is relatively strong and absent.

At pH* 7.1, $[H_2O_2]$ = 2 mM (Figure 3A), only one oxygen-isotope-sensitive band appeared at 789 cm^{-1}, and the 808 cm^{-1} species was completely absent. Nevertheless, the difference between the H_2O_2-treated and ferric pulsed forms at pH* 7.1, $[H_2O_2]$ = 2 mM yielded an intense band at 1503 cm^{-1} as delineated by spectrum D in Figure 7. The peak position and intensity of the band at 1503 cm^{-1} are

[5] A redox-active tyrosine located at position of 160 of subunit D1 or tyrosine 161 of subunit D2 of photosystem II.

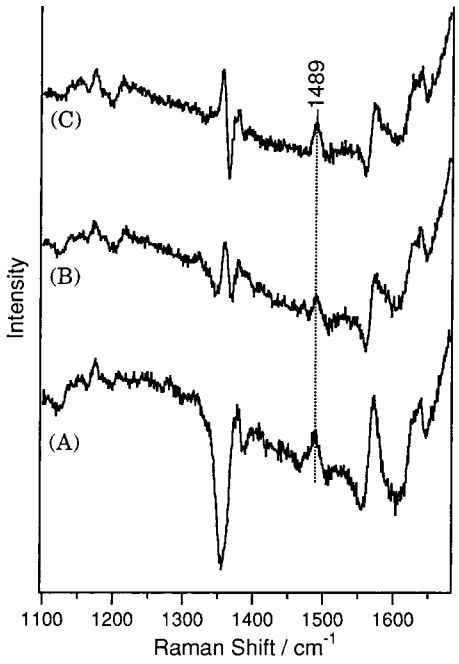

FIGURE 8: Double difference spectra between the H_2O_2-treated minus ferric pulsed forms obtained under different solvent conditions. (A) Difference between the H_2O_2-treated/ferric pulsed difference at pH 10.0, $[H_2O_2] = 0.5$ mM *minus* H_2O_2-treated/ferric pulsed difference at pH* 7.1, $[H_2O_2] = 2$ mM; (B) difference between the H_2O_2-treated/ferric pulsed difference at pH* 9.5, $[H_2O_2] = 2$ mM *minus* H_2O_2-treated/ferric pulsed difference at pH* 7.1, $[H_2O_2] = 2$ mM; (C) difference between the H_2O_2-treated/ferric pulsed difference at pH 9.3, $[H_2O_2] = 2$ mM *minus* H_2O_2-treated/ferric pulsed difference at pH* 7.1, $[H_2O_2] = 2$ mM. The experimental conditions are the same as those in Figure 7.

almost identical to those of spectrum C. Therefore, it is concluded that the 1503 cm^{-1} band is not unique to the 808 cm^{-1} species.

Both difference spectra should represent the spectrum of the Fe^{IV}═O heme *minus* Fe^{III}−heme in addition to possible contributions from the protein moiety. Spectrum D is expected to have no contribution from the protein moiety, since it does not have the 808 cm^{-1} band at all. In fact, the intensity of the 1503 cm^{-1} band appears different between spectra C and D. Accordingly, the double difference was calculated by subtracting spectrum D from spectrum C. The result gave a broad band at 1489 cm^{-1} as delineated by spectrum A in Figure 8. The double difference spectrum is expected to provide a unique vibration of the protein moiety of the 808 cm^{-1} species. The center frequency of the band is close to those previously reported for the C−O stretching mode of a neutral tyrosyl radical (*71*−*74*). To confirm that this is not an artifact of difference calculations, similar double difference spectra were calculated for other combinations in which the P species is stronger. Spectra B and C in Figure 8 display the double difference spectra for pH 9.3, $[H_2O_2] = 2$ mM/ferric pulsed form and for pH* 9.5, $[H_2O_2] = 2$ mM/ferric pulsed form *minus* spectrum D in Figure 7, respectively. All gave a peak at 1489 cm^{-1}. Accordingly, it became more reliable that the 808 cm^{-1} species is accompanied by the 1489 cm^{-1} band from the protein moiety. The intensity of the 1489 cm^{-1} band was weaker in the corresponding double difference spectra excited at 413.1 nm (data not shown). This is reasonable if the absorption peak of the radical is also located around 408−410 nm.

To assign the 1489 cm^{-1} band to a tyrosine radical confidently, it is highly desirable to carry out a mutation experiment. However, when Tyr288 was replaced with Phe, Cu_B was lost and the enzyme was inactive (*75*). We tried to prepare Tyr-d_4-labeled cytochrome *bo* by growing auxotrophic strains of *E. coli* in the medium containing Tyr-d_4. Unfortunately, instability of the protein prepared in this way prevented us from obtaining high-quality RR spectra at high pH and thus assigning the 1489 cm^{-1} band to the tyrosine radical. In this sense, conclusive evidence is lacking at this moment. Nevertheless, it is most likely from the present results that the 808 cm^{-1} species, which we assigned to the P intermediate, contains a tyrosyl radical at the active site.[6]

In summary, we observed three oxygen-isotope-sensitive Raman bands at 805/*X*, 783/753, and (767)/730 cm^{-1} in the reaction of the ferric pulsed form of cytochrome *bo* with H_2O_2. The former two are assigned to the Fe═O stretching mode of the P and F′ forms, respectively. For the P species, the C−O stretching mode of the neutral tyrosyl radical seemed to appear at 1489 cm^{-1}, although it was indirect evidence obtained from difference spectra. Although the intermediates are for the peroxide reaction, they are presumably the same as those in the catalytic reduction of dioxygen by cytochrome *bo*. The (767)/730 cm^{-1} species has been found for the first time in the reaction of terminal oxidases, and its characterization needs more studies.

[6] We could not observe the C−O stretching mode of a tyrosinate around ~1250 cm^{-1}.

ACKNOWLEDGMENT

We are grateful to Dr. T. Matsui of the Institute for Molecular Science for synthesis and a gift of $H_2{}^{18}O_2$, to Dr. M. Tanaka of Kyoto University for a gift of a part of $H_2{}^{18}O_2$, and to Dr. E. H. Appelman of Argonne National Laboratory for a gift of $H_2{}^{16}O{}^{18}O$. We also thank Drs. P. R. Rich and J. A. Moody of University College for providing us a protocol for the preparation of the ferric pulsed cytochrome *bo*, and Drs. T. Ogura, S. Takahashi, and S. Hirota for their stimulating discussions.

REFERENCES

1. Mogi, T., Tsubaki, M., Hori, H., Miyoshi, H., Nakamura, H., and Anraku, Y. (1998) *J. Biochem. Mol. Biol. Biophys. 2*, 79−110.
2. Trumpower, B. L., and Gennis, R. B. (1994) *Annu. Rev. Biochem. 63*, 675−716.
3. Saraste, M., Holm, L., Lemieux, L., Lubben, M., and van der Oost, J. (1991) *Biochem. Soc. Trans. 19*, 608−612.
4. Iwata, S., Ostermeier, C., Ludwig, B., and Michel, H. (1995) *Nature (London) 376*, 660−669.
5. Tsukihara, T., Aoyama, H., Yamashita, E., Tomizaki, T., Yamaguchi, H., Shinzawa-Itoh, K., Nakashima, R., Yaono, R., and Yoshikawa, S. (1996) *Science 272*, 1136−1144.
6. Abramson, J., and Iwata, S. (1998) *EBEC Short Rep. 10*, 81.
7. Wilmanns, M., Lappalainen, P., Kelly, M., Sauer-Eriksson, E., and Saraste, M. (1995) *Proc. Natl. Acad. Sci. U.S.A. 92*, 11955−11959.
8. Kumar, C., Naqui, A., and Chance, B. (1984) *J. Biol. Chem. 259*, 11668−11671.
9. Orii, Y. (1988) *Ann. N.Y. Acad. Sci. 550*, 105−117.

10. Babcock, G. T., and Wikström, M. (1992) *Nature (London) 356*, 301−309.
11. Verkhovsky, M. I., Morgan, J. E., Puustinen, A., and Wikström, M. (1996) *Biochemistry 35*, 16241−16246.
12. Wikstrom, M. (1984) *Nature (London) 308*, 558−560.
13. Brzezinski, P., and Ädelroth, P. (1998) *J. Bioenerg. Biomembr. 30*, 99−107.
14. Michel, H. (1998) *Proc. Natl. Acad. Sci. U.S.A. 95*, 12819−12824.
15. Verkhorsky, M. I., Jasaitis, A., Verkhorskaya, M. L., Morgan, J. E., and Wikstrom, M. (1999) *Nature (London) 400*, 480−482.
16. Ferguson-Miller, S., and Babcock, G. T. (1996) *Chem. Rev. 96*, 2889−2907.
17. Morgan, J. E., Verkhovsky, M. I., and Wikström, M. (1996) *Biochemistry 35*, 12235−12240.
18. Kitagawa, T., and Ogura, T. (1997) *Prog. Inorg. Chem. 45*, 431−479.
19. Ogura, T., Hirota, S., Proshlyakov, D. A., Shinzawa-Itoh, K., Yoshikawa, S., and Kitagawa, T. (1996) *J. Am. Chem. Soc. 118*, 5443−5449.
20. Han, S., Ching, Y. C., and Rousseau, D. L. (1990) *Nature (London) 348*, 89−90.
21. Varotsis, C., and Babcock, G. T. (1995) *J. Am. Chem. Soc. 117*, 11260−11269.
22. Hirota, S., Mogi, T., Ogura, T., Hirano, T., Anraku, Y., and Kitagawa, T. (1994) *FEBS Lett. 352*, 67−70.
23. Proshlyakov, D. A., Ogura, T., Shinzawa-Itoh, K., Yoshikawa, S., and Kitagawa, T. (1996) *Biochemistry 35*, 8580−8586.
24. Wrigglesworth, J. M. (1984) *Biochem. J. 217*, 715−719.
25. Konstantinov, A. A., Capitanio, N., Vygodina, T. V., and Papa, S. (1992) *FEBS Lett. 312*, 71−74.
26. Vygodina, T. V., and Konstantinov, A. A. (1988) *Ann. N.Y. Acad. Sci. 550*, 124−138.
27. Weng, L. C., and Baker, G. M. (1991) *Biochemistry 30*, 5727−5733.
28. Proshlyakov, D. A., Ogura, T., Shinzawa-Itoh, K., Yoshikawa, S., Appelman, E. H., and Kitagawa, T. (1994) *J. Biol. Chem. 269*, 29385−29388.
29. Varotsis, C., Zhang, Y., Appelman, E. H., and Babcock, G. T. (1993) *Proc. Natl. Acad. Sci. U.S.A. 90*, 237−241.
30. Proshlyakov, D. A., Ogura, T., Shinzawa-Itoh, K., Yoshikawa, S., and Kitagawa, T. (1996) *Biochemistry 35*, 76−82.
31. Tsubaki, M., Mogi, T., Anraku, Y., and Hori, H. (1993) *Biochemistry 32*, 6065−6072.
32. Moody, A. J., and Rich, P. R. (1994) *Eur. J. Biochem. 226*, 731−737.
33. Sawaki, Y., and Foote, C. S. (1979) *J. Am. Chem. Soc. 101*, 6292−6296.
34. Pesez, M., and Bartos, J. (1974) *Calorimetric and Fluorimetric Analysis of Organic Compounds and Drugs*, Marcel Dekker, Inc., New York.
35. Hashimoto, S., Teraoka, J., Inubushi, T., Yonetani, T., and Kitagawa, T. (1986) *J. Biol. Chem. 261*, 11110−11118.
36. Reczek, C. M., Sitter, A. J., and Terner, J. (1989) *J. Mol. Struct. 214*, 27−41.
37. Hashimoto, S., Tatsuno, Y., and Kitagawa, T. (1986) *Proc. Natl. Acad. Sci. U.S.A. 83*, 2417−2421.
38. Proniewicz, L. M., Paeng, I. R., and Nakamoto, K. (1991) *J. Am. Chem. Soc. 113*, 3294−3303.
39. Mukai, M., Nagano, S., Tanaka, M., Ishimori, K., Morishima, I., Ogura, T., Watanabe, Y., and Kitagawa, T. (1997) *J. Am. Chem. Soc. 119*, 1758−1766.
40. Sitter, A. J., Reczek, C. M., and Terner, J. (1985) *J. Biol. Chem. 260*, 7515−7522.
41. Tsubaki, M., Mogi, T., Hori, H., Hirota, S., Ogura, T., Kitagawa, T., and Anraku, Y. (1994) *J. Biol. Chem. 269*, 30861−30868.
42. Wang, J., Rumbley, J.. Ching, Y. C., Takahashi, S., Gennis, R. B., and Rousseau, D. L., (1995) *Biochemistry 34*, 15504−15511.
43. Uno, T., Mogi, T., Tsubaki, M., Nishimura, Y., and Anraku, Y. (1994) *J. Biol. Chem. 269*, 11912−11920.
44. Evangelista-Kirkup, R., Smulevich, G., and Spiro, T. G. (1986) *Biochemistry 25*, 4420−4425.
45. Ramsden, J., and Spiro, T. G. (1989) *Biochemistry 28*, 3125−3127.
46. Hill, J., Goswitz, V. C., Calhoun, M., Garcia-Horsman, J. A., Lemieux, L., Alben, J. O., and Gennis, R. B. (1992) *Biochemistry 31*, 11435−11440.
47. Mitchell, D. M., Shapleigh, J. P., Archer, A. M., Alben, J. O., and Gennis, R. B. (1996) *Biochemistry 35*, 9446−9450.
48. Watmough, N. J., Cheesman, M. R., Greenwood, C., and Thomson, A. J. (1994) *Biochem. J. 300*, 469−475.
49. Brittain, T., Little, R. H., Greenwood, C., and Watmough, N. J. (1996) *FEBS Lett. 399*, 21−25.
50. Cheesman, M. R., Watmough, N. J., Gennis, R. B., Greenwood, C., and Thomson, A. J. (1994) *Eur. J. Biochem. 219*, 595−602.
51. Oertling, W. A., Kean, R. T., Wever, R., and Babcock, G. T. (1990) *Inorg. Chem. 29*, 2633−2645.
52. Kahlow, M. A., Zuberi, T. M., Gennis, R. B., and Loehr, T. M. (1991) *Biochemistry 30*, 11485−11489.
53. Schappacher, M., Chottard, G., and Weiss, R. (1986) *J. Chem. Soc., Chem. Commun.*, 93−94.
54. Kitagawa, T. (1988) *Biological Applications of Raman Spectroscopy* (Spiro, T. G., Ed.) Vol. III, pp 97−132, John Wiley & Sons, New York.
55. Mogi, T., Nakamura, H., and Anraku, Y. (1994) *J. Biochem. (Tokyo) 116*, 471−477.
56. Mogi, T., Minagawa, J., Hirano, T., Sato-Watanabe, M., Tsubaki, M., Uno, T., Hori, H., Nakamura, H., Nishimura, Y., and Anraku, Y. (1998) *Biochemistry 37*, 1632−1639.
57. Proshlyakov, D. A., Pressler, M. A., and Babcock, G. T. (1998) *Proc. Natl. Acad. Sci. U.S.A. 95*, 8020−8025.
58. Gennis, R. B. (1998) *Biochim. Biophys. Acta 1365*, 241−248.
59. MacMillan, F., Kannt, A., Behr, J., Prisner, T., and Michel, H. (1999) *Biochemisry 38*, 9179−9183.
60. Yoshikawa, S., Shinzawa-Itoh, K., Nakashima, R., Yaono, R., Yamashita, E., Inoue, N., Yao, M., Fei, M. J., Libeu, C. P., Mizushima, T., Yamaguchi, H., Tomizaki, T., and Tsukihara, T. (1998) *Science 280*, 1723−1729.
61. Ostermeier, C., Harrenga, A., Ermler, U., and Michel, H. (1997) *Proc. Natl. Acad. Sci. U.S.A. 94*, 10547−10553.
62. Sundaramoorthy, M., Terner, J., and Poulos, T. L. (1995) *Structure 3*, 1367−1377.
63. Karthein, R., Dietz, R., Nastainczyk, W., and Ruf, H. H. (1988) *Eur. J. Biochem. 171*, 321−328.
64. Barry, B. A., and Babcock, G. T. (1987) *Proc. Natl. Acad. Sci. U.S.A. 84*, 7099−7103.
65. Debus, R. J., Barry, B. A., Babcock, G. T., and McIntosh, L. (1988) *Proc. Natl. Acad. Sci. U.S.A. 85*, 427−430.
66. Hays, A. M., Vassiliev, I. R., Golbeck, J. H., and Debus, R. J. (1998) *Biochemistry 37*, 11352−11365.
67. Diner, B. A., Force, D. A., Randall, D. W., and Britt, R. D. (1998) *Biochemistry 37*, 17931−17943.
68. Ahlbrink, R., Haumann, M., Cherepanov, D., Bogershausen, O., Mulkidjanian, A., and Junge, W. (1998) *Biochemistry 37*, 1131−1142.
69. Chen, Y. R., Gunther, M. R., and Mason, R. P. (1999) *J. Biol. Chem. 274*, 3308−3314.
70. Liu, A., Potsch, S., Davydov, A., Barra, A. L., Rubin, H., and Graslund, A. (1998) *Biochemistry 37*, 16369−16377.
71. Backes, G., Sahlin, M., Sjöberg, B. M., Loehr, T. M., and Sanders-Loehr, J. (1989) *Biochemistry 28*, 1923−1929.
72. Kim, S., Ayala, I., Steenhuis, J. J., Gonzalez, E. T., Razeghifard, M. R., and Barry, B. A. (1998) *Biochim. Biophys. Acta 1366*, 331−354.
73. Tripathi, G. N. R., and Schuler, R. H. (1984) *J. Chem. Phys. 81*, 113−121.
74. Itoh, S., Taki, M., Takayama, S., Nagatomo, S., Kitagawa, T., Sakurada, N., Arakawa, R., and Fukuzumi, S. (1999) *Angew. Chem., Int. Ed. Engl. 38*, 2774−2776.
75. Kawasaki, M., Mogi, T., and Anraku, Y. (1997) *J. Biochem. (Tokyo) 122*, 422−429.

BI992538R